

Weak Ferromagnetism in $\text{Fe}_{1-x}\text{Co}_x\text{Sb}_2$

Rongwei Hu^{1,2}, R. P. Hermann^{3*}, F. Grandjean³, Y. Lee⁴, J. B. Warren⁵, V. F. Mitrović² and C. Petrović¹

¹*Condensed Matter Physics, Brookhaven National Laboratory, Upton New York 11973-5000 USA*

²*Physics Department, Brown University, Providence RI 02912*

³*Department of Physics B5, Université de Liège, Belgium*

⁴*Department of Earth System Sciences, Yonsei University, Seoul 120749, Korea*

⁵*Instrumentation Division, Brookhaven National Laboratory, Upton New York 11973-5000 USA*

(Dated: October 24, 2018)

Weak ferromagnetism in $\text{Fe}_{1-x}\text{Co}_x\text{Sb}_2$ is studied by magnetization and Mössbauer measurements. A small spontaneous magnetic moment of the order of $\sim 10^{-3}\mu_B$ appears along the \hat{b} -axis for $0.2 \leq x \leq 0.4$. Based on the structural analysis, we argue against extrinsic sources of weak ferromagnetism. We discuss our results in the framework of the nearly magnetic electronic structure of the parent compound FeSb_2 .

PACS numbers: 75.30.-m, 76.80.+y, 71.28.+d

I. INTRODUCTION

FeSi and FeSb_2 are semiconductors that show crossover from a nonmagnetic semiconducting ground state with a narrow gap to a thermally induced paramagnetic metal with enhanced susceptibility.^{1,2} The magnetic properties of FeSi have instigated considerable theoretical interest, starting with the narrow-band model of Jaccarino.³ Further models include a nearly ferromagnetic semiconductor model of Takahashi and Moriya⁴ in which the state was sustained by thermally induced spin fluctuations found in neutron scattering experiments.^{5,6} Moreover, the nearly ferromagnetic semiconductor picture was supported by $LDA+U$ band structure calculations by Mattheiss and Hamann⁷ and Anisimov *et al.*⁸ At the same time, Aeppli and Fisk⁹ pointed out that the magnetic properties of FeSi are analogous to the physics of Kondo insulators, albeit with a reduced on-site Coulomb repulsion U . The basis of their argument was a model, ruled out by Jaccarino in his original work, of the narrow gap and high density of states. Experiments of Mandrus *et al.*¹⁰ and Park *et al.*¹¹ confirmed the validity of the model of Aeppli and Fisk.

A search for new model systems, where the applicability of the Kondo insulator framework to $3d$ transition metals can be investigated, led to the synthesis of large single crystals of FeSb_2 . Furthermore, a crossover was discovered similar to the one in FeSi , for the magnetic and electrical transport properties.^{2,12} Subsequent alloying studies have shown heavy fermion metallic state induced in $\text{FeSb}_{2-x}\text{Sn}_x$, just as in $\text{FeSi}_{1-x}\text{Al}_x$.^{13,14} In both materials the optical conductivity revealed unconventional charge gap formation. That is, a complete recovery of spectral weight in FeSi and FeSb_2 occurs over an energy range of few eV, suggesting contributions of larger energy scales.^{15,16} This is in sharp contrast to metal-insulator transitions in band insulators where thermal excitations of charge carriers through the gap redistribute just above the gap.

One of the key predictions of the $LDA+U$ approach was the close proximity of FeSi to a ferromagnetic state.¹⁷

In analogy to FeSi , recent ab-initio calculations predicted the nearly ferromagnetic nature of the FeSb_2 ground state.¹⁸ In FeSi the ferromagnetic state has been induced by lattice expansion in $\text{FeSi}_{1-x}\text{Ge}_x$ ¹⁹ or by carrier insertion in $\text{Fe}_{1-x}\text{Co}_x\text{Si}$.²⁰ In contrast, FeSb_2 has not yet been tuned to a ferromagnetic state by any external parameters. In this work, we demonstrate the presence of the weak ferromagnetism (WFM) in $\text{Fe}_{1-x}\text{Co}_x\text{Sb}_2$ ($0.2 \leq x \leq 0.45$). The origins of the WFM are discussed. Extensive structural analysis shows no evidence of extrinsic impurity induced WFM. We argue that instead the WFM is a consequence of the nearly ferromagnetic electronic structure of the parent compound FeSb_2 .

II. EXPERIMENT

The $\text{Fe}_{1-x}\text{Co}_x\text{Sb}_2$ single crystals were grown from excess Sb flux.² Powder X-ray diffraction (XRD) patterns of the ground samples were taken with $\text{Cu K}\alpha$ radiation ($\lambda = 1.5418 \text{ \AA}$) using a Rigaku Miniflex X-ray diffractometer. The lattice parameters were obtained using Rietica software.²¹ High resolution XRD patterns were taken at the beamline X7A of the National Synchrotron Light Source at the Brookhaven National Laboratory using monochromatic synchrotron X-ray and gas-proportional position-sensitive detector. Rietveld refinements were performed using GSAS.²² A JEOL JSM-6500 SEM microprobe with resolution of 1.5 nm was used for verifying the Co concentrations and investigating the microstructure. Single crystals were oriented using a Laue Camera. Magnetization measurements were performed in a Quantum Design MPMS XL 5 instrument. The iron-57 Mössbauer spectra, at temperatures ranging from 2.8 to 295 K, were measured on a constant acceleration spectrometer that utilized a rhodium matrix cobalt-57 source. The instrument was calibrated at 295 K with α -iron powder. The isomer shifts reported herein are relative to α -iron at 295 K. The thickness of the absorber was 23 and 72 mg/cm^2 for FeSb_2 and $\text{Fe}_{0.75}\text{Co}_{0.25}\text{Sb}_2$, respectively. The sample temperature in the Janis SV-300

cryostat was controlled with a LakeShore 330 temperature controller and a silicon diode mounted on the copper sample holder. The accuracy of the sample temperature is better than $\pm 1\%$.

The powder X-ray patterns show that the $\text{Fe}_{1-x}\text{Co}_x\text{Sb}_2$ ($0.2 \leq x \leq 0.45$) samples crystallize in the $Pnmm$ structure without any additional crystalline peaks introduced by Co alloying. The effect of Co substitution on the Fe site is to expand the unit cell volume as compared to FeSb_2 . This expansion is anisotropic and results from a contraction in the basal a - b plane and an expansion along the c -axis upon substitution of Fe by Co.²³

III. MAGNETIC PROPERTIES

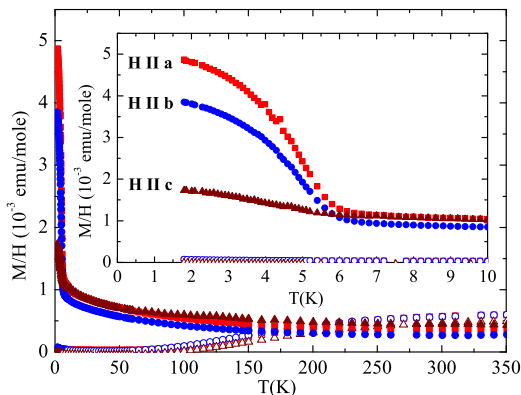


FIG. 1: Magnetic susceptibility M/H of FeSb_2 (open symbols) and $\text{Fe}_{0.75}\text{Co}_{0.25}\text{Sb}_2$ (filled symbols) for a 1 kOe field applied along all three principal crystalline axes.

At low temperature, the parent compound FeSb_2 is a narrow gap semiconductor with a rather small and temperature independent magnetic susceptibility.² Similar to FeSi , above 100 K there is a temperature induced paramagnetic susceptibility and an enhanced electronic conduction. The magnetic susceptibility can be described by both a thermally induced Pauli susceptibility and a low to high spin transition.^{2,12,25} In the temperature (T) range from 1.7 to 150 K the $\text{Fe}_{0.75}\text{Co}_{0.25}\text{Sb}_2$ magnetic susceptibility is larger than that of FeSb_2 . For T above 6 K, it shows little anisotropy with the magnetic field applied along the different crystallographic axes. As shown in Fig. 1, the temperature dependence of the susceptibility indicates Pauli paramagnetism at high temperature. A clear ferromagnetic transition at $T_C = 6$ K for a field of 1 kOe applied along any of the three crystallographic axes is illustrated in the inset to Fig. 1. These observations are in agreement with ferromagnetic long range order of the small magnetic moments below $T = 5$ K.²³ The ferromagnetic nature of the transition is supported by the hysteresis loop measured at $T = 1.8$ K and displayed in

Fig. 2. For field strength varying between -6 and 6 kOe applied along the \hat{b} -axis, hysteresis loops are observed for $0.20 \leq x \leq 0.45$. The width of the hysteresis loop grows initially with increasing x from $x = 0.20$, peaks at $x = 0.25$, and becomes progressively smaller upon further Co substitution. Hysteresis loops are absent for field applied along the \hat{c} -axis and are observed only for $x = 0.25$ for field applied along the \hat{a} -axis. By extrapolating the magnetization of $\text{Fe}_{0.75}\text{Co}_{0.25}\text{Sb}_2$ to $H=0$, a lower estimate of the saturation magnetization along the b -axis of $M_{LL} = 0.0005 \mu_B/\text{F.U.}$ (or $5 \cdot 10^{-4} \mu_B/\text{Fe}$), where F.U. refers to the FeSb_2 formula unit, is obtained.

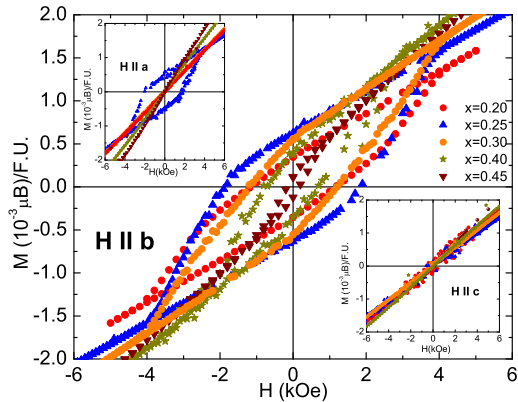


FIG. 2: Hysteresis loops for $\text{Fe}_{1-x}\text{Co}_x\text{Sb}_2$ in the ferromagnetic state ($x = 0.2 - 0.45$) at $T = 1.8$ K. Magnetization does not saturate, it continues to increase with applied magnetic field, similar to bulk itinerant ferromagnets with $3d$ ions.

The Mössbauer spectra of FeSb_2 single crystals exhibit a doublet at $T=295$ and 4.2 K. No impurity, and in particular no impurity with a large hyperfine field, is observed in the Mössbauer spectra. Furthermore, the Mössbauer spectral parameters for FeSb_2 obtained herein are in excellent agreement with the previously reported parameters (see Table I).²⁶ For $\text{Fe}_{0.75}\text{Co}_{0.25}\text{Sb}_2$, the Mössbauer spectra, shown in Fig. 3, exhibit a doublet for temperatures ranging from $T = 295$ K to 2.8 K. Again no impurity contribution is observed. Its spectral parameters, obtained at $T = 295$ K and 4 K, are close to those observed in the FeSb_2 . The isomer shift observed in $\text{Fe}_{0.75}\text{Co}_{0.25}\text{Sb}_2$ is ca. 0.01 mm/s smaller than in FeSb_2 . This indicates a somewhat larger s -electron density at the ^{57}Fe nucleus.

The variation of the quadrupole splitting from 295 to 4.2 K is larger in FeSb_2 than in $\text{Fe}_{0.75}\text{Co}_{0.25}\text{Sb}_2$. This strong temperature dependence of the quadrupole splitting in FeSb_2 is consistent with a scenario of electron delocalization appearing with increasing temperature, with a gap ΔE of 380 K.^{25,27} As illustrated in Fig. 4, a fit of the $\text{Fe}_{0.75}\text{Co}_{0.25}\text{Sb}_2$ quadrupole splitting as a function of temperature with the delocalization model described in Ref. 24 yields a somewhat larger gap energy $E_g = (480 \pm 50)$ K than that observed in FeSb_2 . The dif-

TABLE I: The hyperfine parameters for FeSb_2 and $\text{Fe}_{0.75}\text{Co}_{0.25}\text{Sb}_2$ ^a; ^aRelative to α -iron at 295K and ^bThe isomer shift reference in Ref. 24 is sodium nitroprusside, which has a -0.26 mm/s isomer shift relative to α -iron at room temperature.

T(K)	$\text{Fe}_{0.75}\text{Co}_{0.25}\text{Sb}_2$			FeSb_2		
	δ^a , mm/s	ΔE_Q , mm/s	Γ , mm/s	δ^a , mm/s	ΔE_Q , mm/s	Γ , mm/s
296 ^b	-	-	-	0.450(6)	1.286(6)	-
295	0.433(2)	1.343(2)	0.264(5)	0.449(1)	1.275(2)	0.262(3)
240	0.483(2)	1.394(2)	0.265(2)	-	-	-
190	0.509(2)	1.422(2)	0.267(2)	-	-	-
140	0.538(2)	1.449(2)	0.273(2)	-	-	-
90	0.455(2)	1.364(2)	0.284(2)	-	-	-
50	0.569(2)	1.474(3)	0.290(4)	-	-	-
6.4 ^b	-	-	-	0.572(6)	1.575(6)	-
4.2	0.560(2)	1.483(2)	0.291(2)	0.572(1)	1.573(3)	0.270(4)
2.8	0.558(2)	1.483(3)	0.338(4)	-	-	-

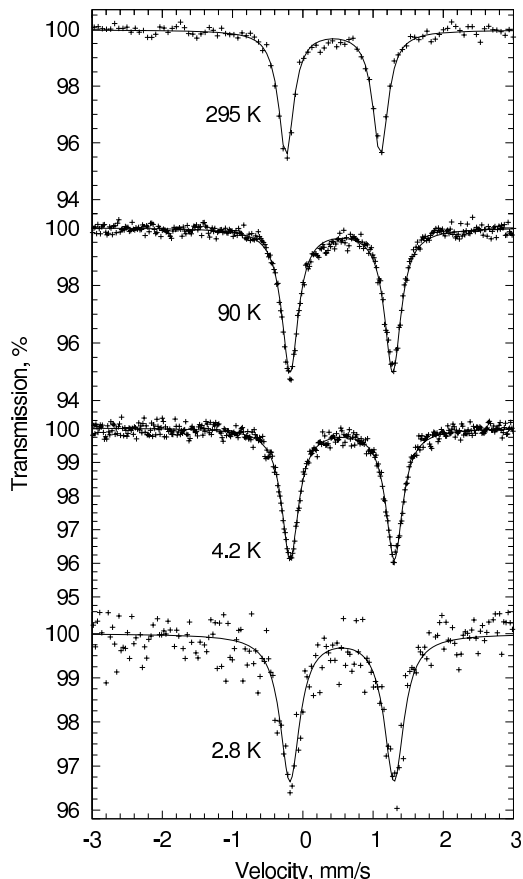


FIG. 3: The ^{57}Fe Mössbauer spectra of $\text{Fe}_{0.75}\text{Co}_{0.25}\text{Sb}_2$ at the indicated temperatures. The solid line is a fit to a doublet, using the parameters indicated in Table 1.

ference between the hyperfine parameters in FeSb_2 and $\text{Fe}_{0.75}\text{Co}_{0.25}\text{Sb}_2$ indicates that there is indeed a modification of the FeSb_2 structure, and that no phase segregation is present. The Mossbauer spectra show that the investigated phase is $(\text{Fe},\text{Co})\text{Sb}_2$ and not $\text{FeSb}_2 + \text{CoSb}_2$ since the hyperfine parameters are significantly differ-

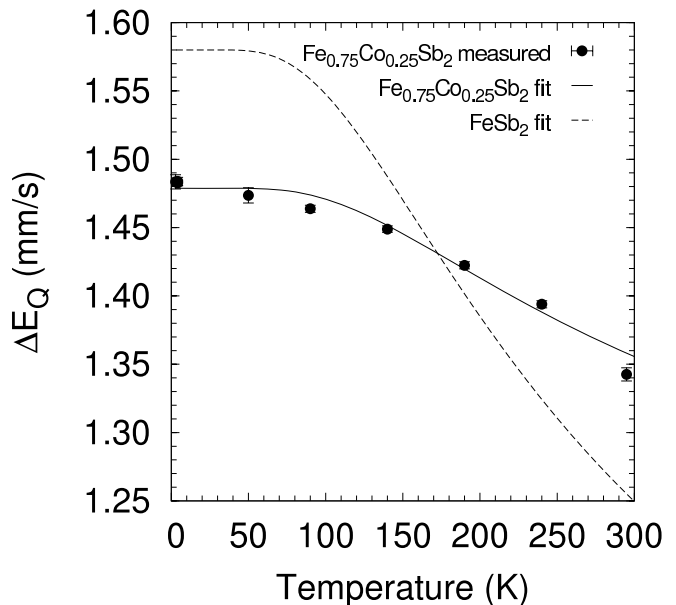


FIG. 4: Fit of the $\text{Fe}_{0.75}\text{Co}_{0.25}\text{Sb}_2$ quadrupole splitting as a function of temperature with the delocalization model.

ent. Furthermore no iron-bearing impurity is observed in $\text{Fe}_{0.75}\text{Co}_{0.25}\text{Sb}_2$.

Apparently, the $T = 2.8$ K spectrum of $\text{Fe}_{0.75}\text{Co}_{0.25}\text{Sb}_2$ is a doublet, which is somewhat surprising. Our interpretation is that either the iron experiences no magnetic hyperfine field or that the hyperfine field is below the detection limit. If the small broadening of ca. 0.047(6) mm/s of the 2.8 K spectrum, when compared to the 4.2 K spectrum, was associated to a magnetic hyperfine field, it would correspond to a 1.5 \pm 0.2 kOe hyperfine field. With a linewidth constrained to 0.29 mm/s, a fit of this spectrum, with both a quadrupole interaction and a hyperfine field yields a field of 2.8 \pm 1.2 kOe. Taking the usual proportionality of ca. 150 kOe/ μ_B , these values can be used to estimate an upper limit of about $M_{UL} = 0.01 \mu_B$. for the magnetic moment on Fe.

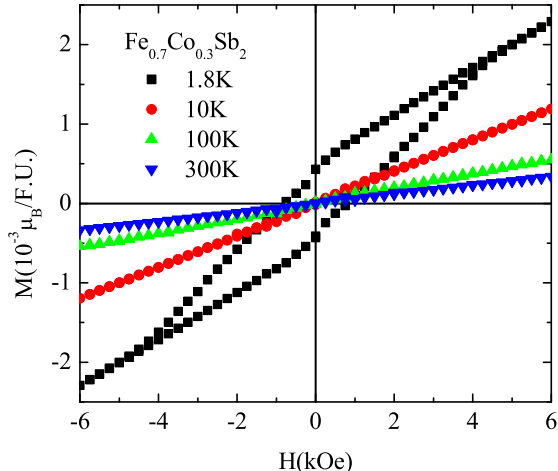


FIG. 5: Magnetic hysteresis for the $\text{Fe}_{0.7}\text{Co}_{0.3}\text{Sb}_2$ sample. It is important to note the absence of hysteresis loops above the ferromagnetic transition of FeSb_2 . Data were taken on a crystal from independently grown batch.

IV. INTRINSIC VS. EXTRINSIC MAGNETISM

Given the small value of the saturated moment, it is possible that WFM originates from extrinsic sources, such as artifacts of the measurement process or the presence of a small amount of ferromagnetic impurity, e.g. elemental Fe. The former can be excluded based on the lack of sample dependence, both in magnetization and in heat capacity data.²³ Below we discuss the possibility of undetected second phases as extrinsic sources of the WFM.

No hysteresis loops are observed for temperatures above $T_C = (6 - 7)K$ for $x = (0.2 - 0.4)$ (example shown in Fig. 5). No known Fe-Sb, Co-Sb, Fe-Co, Fe-O, or Co-O phases show a ferromagnetic transition in this temperature range. FeCo alloys have large hyperfine fields (200-400 kOe) that would have been detected by Mössbauer measurement. We can calculate the X-ray patterns expected in the presence of bulk crystalline Fe impurities by superimposing the strongest peak of 0.3% elemental Fe to the measured patterns. No overlap between the calculated and measured $\text{Fe}_{0.75}\text{Co}_{0.25}\text{Sb}_2$ X-ray patterns was observed (Fig. 6). Any other unknown Fe-O, Fe-Co-O, Co-O, Fe-Co, Fe-Sb-Co, *etc.* phase with the same atomic ratio in the mixture would have been detected and refined by synchrotron powder X-ray diffraction because its contribution to the scattering mixture would be higher than that of Fe. Though M_{LL} observed in magnetic hysteresis loops could be caused by Fe impurities of the order of the synchrotron powder X-ray diffraction detection limit, absence of hysteresis loops above 6 K strongly argues against such scenario.

Another possibility is that magnetism in $\text{Fe}_{1-x}\text{Co}_x\text{Sb}_2$

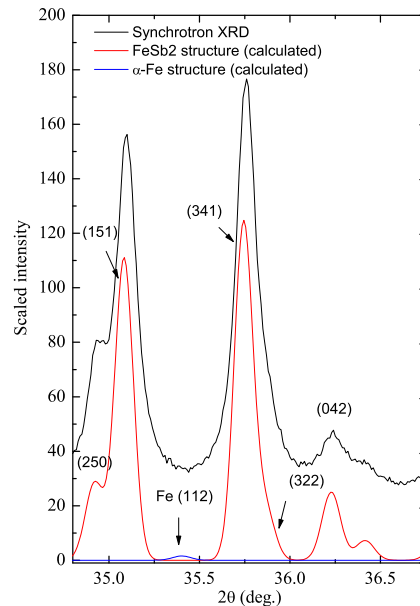


FIG. 6: Observed (black) and calculated (red) synchrotron powder X-ray diffraction patterns of $\text{Fe}_{0.75}\text{Co}_{0.25}\text{Sb}_2$. Calculated pattern includes 0.3 % of superimposed α -Fe impurity. If present, impurity would have caused detectable deviation of the observed pattern since there is no peak overlap.

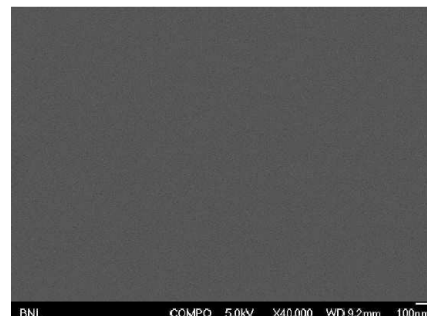


FIG. 7: Typical Scanning Electron Microscope (SEM) image of $\text{Fe}_{0.75}\text{Co}_{0.25}\text{Sb}_2$. SEM images on randomly chosen surface did not detect secondary phases or randomly distributed nanoparticles.

is caused by magnetic nanoparticles. Mössbauer measurement shows no evidence of iron bearing nanoparticles (either FeCo or Fe-oxide). Such nanoparticles would have a paramagnetic spectrum with different isomer shift and quadrupole splitting at room temperature, which would be detected with a 0.3% limit. Below the nanoparticle blocking temperature the field would be large, typically 500 kOe for typical oxides. Solid evidence against nanoparticles or bulk extrinsic phases comes from energy dispersive scanning electron microscope (SEM) measurements. Among the samples grown from several different batches for $x = 0.25$, the uncertainty in Co concentration is $x = 0.04$. SEM data taken with resolution down to 1.5 nm exclude the presence of either bulk secondary phases

or embedded nanoparticles. This is because high resolution SEM images of several randomly chosen polished crystals and crystalline surfaces show no trace of nanosize inclusions, clusters or inhomogeneities (example shown in Fig. 7). The images were taken in the “composition” mode with a solid state detector consisting of paired PN junctions. This type of detector is very sensitive to back-scattered electrons which in turn are sensitive to local variations in atomic number. If nano-crystallites of Fe or other elements were present, they would have been visible as bright dots in the high magnification image.

Taken in conjunction, our results argue against extrinsic sources of WFM in $\text{Fe}_{1-x}\text{Co}_x\text{Sb}_2$. Recent muon spin relaxation measurements indicate that the WFM state is spread throughout the full sample volume for $\text{Fe}_{0.7}\text{Co}_{0.3}\text{Sb}_2$, further supporting our results.²⁸

V. DISCUSSION AND CONCLUSIONS

Examples of intrinsic WFM states in narrow band materials are abundant in nature.²⁹ Besides numerous oxide compounds, many intermetallic systems also exhibit intrinsic weak ferromagnetism, such as YbRhSb ,³⁰ MnS ,³¹ and $\text{Yb}_{0.8}\text{Y}_{0.2}\text{InCu}_4$.³² Magnetism in FeSb_2 in analogy to FeSi has been predicted by $LDA+U$ calculations.¹⁸ Besides the use of an external magnetic field, one interesting possibility would be to induce the ferromagnetic state by lattice expansion and band narrowing, as in $\text{FeSi}_{1-x}\text{Ge}_x$.^{19,34} Unfortunately, isoelectronic lattice expansion is limited to rather small values of x in $\text{FeSb}_{2-x}\text{Bi}_x$. Our preliminary data show that the ferromagnetic state is not reached for $x = 0.016$. As in $\text{Fe}_{1-x}\text{Co}_x\text{Si}$, ferromagnetic state is induced with Co substitution in FeSb_2 . In both alloy systems critical temperature T_C exhibits a characteristic peak as a function of Co concentration.^{23,24} Whereas metallicity simultaneously appears with ferromagnetism in $\text{Fe}_{1-x}\text{Co}_x\text{Si}$ at $x = 0.05$,²⁰ in $\text{Fe}_{1-x}\text{Co}_x\text{Sb}_2$ alloys transport and spin gap vanish at $x = 0.1$ and $x = 0.2$ respectively.²³

What could be the mechanism of the WFM in $\text{Fe}_{1-x}\text{Co}_x\text{Sb}_2$ alloys? Knowing that there is an inversion symmetry at the Fe site in the $Pn\bar{m}$ space group of FeSb_2 , we can exclude the presence of the Dzyaloshinskii - Moriya (DM) type of interactions. This is in contrast to the doped FeSi where the DM interaction is believed to be responsible for the WFM.^{33,34} A canted antiferromagnetism can be excluded based on the observed field dependence of the transition temperature. That is, the ferromagnetic tail at low temperature is insensitive to

variation of the applied field. However, it is possible to ascribe the low magnetic moment in Co doped FeSb_2 to the partial ordering of Co^{2+} ions. This scenario is in agreement with detailed analysis of the magnetic and thermodynamic properties of $\text{Fe}_{1-x}\text{Co}_x\text{Sb}_2$.²³

Besides the obvious lattice expansion, the effect of the Co insertion is to introduce extra carriers in the system. The carriers cause a closing of the gap by $x = 0.1$.²³ Thus, the WFM appearance could be a consequence of carrier-induced metallicity. This claim is further supported by discarding another well known scenario for the WFM induction. More precisely, one can imagine that the WFM is induced by an “inverted metal-insulator” scenario.^{17,34} In this scenario, magnetic order exists only in the metallic phase. Furthermore, the metallicity is a direct consequence of transition to the ferromagnetic state where a bulk moment of $\sim 1\mu_B$ develops out of small gap semiconductor with small susceptibility.^{17,34} However, in $\text{Fe}_{1-x}\text{Co}_x\text{Sb}_2$ for $x = 0.2 - 0.45$ a small ordered moment is induced. Therefore, the presence of the small moment excludes the “inverted metal-insulator” scenario and leaves as the only possibility that the WFM arises as a consequence of carrier-induced metallicity.

In conclusion, detailed structural and magnetic measurements argue against extrinsic sources of WFM in Co - substituted FeSb_2 . The ordered moment below the WFM transition for $\text{Fe}_{0.75}\text{Co}_{0.25}\text{Sb}_2$ is $M \sim (0.5 - 10) \cdot 10^{-3}\mu_B/\text{Fe}$. As opposed to FeSi where the metallic state is caused by band narrowing of nearly ferromagnetic parent electronic structure, weak ferromagnetism in $\text{Fe}_{1-x}\text{Co}_x\text{Sb}_2$ could be a consequence of carrier induced metallic state. In order to fully understand the magnetic structure, magnitude of moments, and mechanism of magnetic ordering, further neutron scattering and/or nuclear magnetic resonance measurements are envisaged.

We thank Yasutomo Uemura, Paul Canfield, T. M. Rice and Maxim Dzero for useful communications and Dr. L. Rebbouh for assistance in the Mössbauer spectral measurements. This work was carried out at the Brookhaven National Laboratory which is operated for the U.S. Department of Energy by Brookhaven Science Associates (DE-Ac02-98CH10886), and at Department of Physics, Université de Liège, Belgium. This work was also supported in part by the National Science Foundation DMR-0547938 (V. F. M.).

*Present address: Institut für Festkörperforschung, Forschungszentrum Jülich GmbH, D-52425 Jülich, Germany

¹ F. Hulliger, Nature (London), **198**, 1081 (1963).

² C. Petrovic, J. W. Kim, S. L. Bud'ko, A. I. Goldman, P. C. Canfield, W. Choe and G. J. Miller, Phys. Rev. B **67**, 155205 (2003).

³ V. Jaccarino, G. K. Wertheim, J. H. Werinick, L. R. Walker

and S. Arajs, Phys. Rev. **160**, 476 (1967).

⁴ Y. Takahashi and T. Moriya, J. Phys. Soc. Jpn. **46**, 1451 (1979).

⁵ G. Shirane, J. E. Fischer, Y. Endoh and K. Tajima, Phys. Rev. Lett. **59**, 351 (1987).

- ⁶ K. Tajima, Y. Endoh, J. E. Fischer and G. Shirane, *Phys. Rev. B* **38**, 6954 (1988).
- ⁷ L. F. Mattheis and D. R. Hamann, *Phys. Rev. B* **47**, 13114 (1993).
- ⁸ V. I. Anisimov, J. Zaanen and O. K. Anderson, *Phys. Rev. B* **44**, 943 (1991).
- ⁹ G. Aeppli and Z. Fisk, *Comments Cond. Mat. Phys.* **16**, 155 (1992).
- ¹⁰ D. Mandrus, J. L. Sarrao, A. Migliori, J. D. Thompson, and Z. Fisk, *Phys. Rev. B* **51**, 4763 (1995).
- ¹¹ C.-H. Park, Z.-X. Shen, A. G. Loeser, D. S. Dessau, D. G. Mandrus, A. Migliori, J. Sarrao, and Z. Risk, *Phys. Rev. B* **52**, 16981 (1995).
- ¹² C. Petrovic, Y. Lee, T. Vogt, N. Dj. Lazarov, S. L. Bud'ko and P. C. Canfield, *Phys. Rev. B* **72**, 045103 (2005).
- ¹³ A. Bentien, G. K. H. Madsen, S. Johnsen, and B. B. Iversen., *Phys. Rev. B* **74**, 205105 (2006).
- ¹⁴ J. F. DiTusa, K. Friemelt, E. Bucher, G. Aeppli and A. P. Ramirez, *Phys. Rev. B* **58**, 10288 (1998).
- ¹⁵ Z. Schlesinger, Z. Fisk, H-T. Zhang, M. B. Maple, J. F. DiTusa and G. Aeppli, *Phys. Rev. Lett.* **71**, 1748 (1993).
- ¹⁶ A. Perucchi, L. Degiorgi, Rongwei Hu, C. Petrovic and V. F. Mitrovic, *European Physical Journal B* **54**, 175 (2006).
- ¹⁷ V. I. Anisimov, S. Yu. Ezhov, I. S. Elfimov, I. V. Solovyev and T. M. Rice, *Phys. Rev. Lett.* **76**, 1735 (1996).
- ¹⁸ A. V. Lukoyanov, V. V. Mazurenko, V. I. Anisimov, M. Sigrist and T. M. Rice, *European Physical Journal B* **53**, 205 (2006).
- ¹⁹ S. Yeo, S. Nakatsuji, A. D. Bianchi, P. Schlotmann, Z. Fisk, L. Balicas, P. A. Stampe and R. J. Kennedy, *Phys. Rev. Lett.* **91**, 046401 (2003).
- ²⁰ N. Manayala, Y. Sidis, J. F. DiTusa, G. Aeppli, D. P. Young and Z. Fisk, *Nature* **404**, 581 (2000).
- ²¹ Hunter B., "Rietica - A visual Rietveld program", International Union of Crystallography Commission on Powder Diffraction Newsletter No. **20**, (Summer) <http://www.rietica.org> (1998).
- ²² A. C. Larson and R. B. VonDreele, (Report LAUR 86-748, Los Alamos National Laboratory, New Mexico, 1986). B. H. Toby, *J. Appl. Crystallogr.* **34**, 210 (2001).
- ²³ Rongwei Hu, V. F. Mitrovic, and C. Petrovic, *Phys. Rev. B* **74**, 195130 (2006).
- ²⁴ S. V. Grigoriev, S. V. Maleyev, V. A. Dyadkin, D. Menzel, J. Schoenes, and H. Eckerlebe, *Phys. Rev. B* **76**, 092407 (2007).
- ²⁵ A. Gérard and F. Grandjean, *J. Phys. Chem. Solids* **36**, 1365 (1975).
- ²⁶ J. Steger and E. Kostiner, *J. Sol. St. Chem.* **5**, 131 (1972).
- ²⁷ J. B. Goodenough, *J. Sol. State Chem.* **5**, 144 (1972).
- ²⁸ T. Uemura, private communication
- ²⁹ L. E. De Long, J. G. Huber and K. S. Bedell, *J. Magn. Magn. Mater* **99**, 171 (1991).
- ³⁰ Y. Muro, Y. Haizaki, M. S. Kim, K. Umeo, H. Tou, M. Sera, and T. Takabatake, *Phys. Rev. B* **69**, 020401 (2004).
- ³¹ S. S. Aplesnin, L. I. Ryabinkina, G. M. Abramova, O. B. Romanova, A. M. Vorotynov, D. A. Velikanov, N. I. Kiselev, and A. D. Balaev, *Phys. Rev. B* **71**, 125204 (2005).
- ³² A. Mitsuda, T. Goto, K. Yoshimura, W. Zhang, N. Sato, K. Kosuge and H. Wada, *J. Phys. Chem. Solids*, **63**, 1211 (2002).
- ³³ B. Lebech, J. Bernhard and T. Freltoft, *J. Phys. Cond. Matter* **1**, 6105 (1989).
- ³⁴ V. I. Anisimov, R. Hlubina, M. A. Korotin, V. Mazurenko, T. M. Rice, A. O. Shorikov and M. Sigrist, *Phys. Rev. Lett.* **89**, 257203 (2002).